

# Assignment of Protoheme Resonance Raman Spectrum by Heme Labeling in Myoglobin

Songzhou Hu,<sup>†</sup> Kevin M. Smith,<sup>‡</sup> and Thomas G. Spiro<sup>\*,†</sup>

Contribution from the Departments of Chemistry, Princeton University, Princeton, New Jersey 08544, and University of California, Davis, California 95616

Received July 1, 1996<sup>⊗</sup>

**Abstract:** Resonance Raman (RR) spectra are reported for myoglobin reconstituted with seven heme isotopomers which are labeled with <sup>15</sup>N and *meso*-D<sub>4</sub> in the porphyrin skeleton or at the vinyl and propionate substituents. The RR bands are assigned to the porphyrin in-plane and out-of-plane modes as well as to the internal vibrations of substituents on the basis of the observed isotope shifts. The issue of vinyl substituent effects is revisited, and bands are assigned to the 2- or 4-vinyl group from selective deuteration shifts. Contributions of the aliphatic propionate groups are also revealed in the RR spectrum. The protein influence on the heme structure is reflected in the activation of several out-of-plane modes in the low-frequency region.

## Introduction

Resonance Raman (RR) spectroscopy plays a key role in the study of heme proteins because of the strong signal enhancement and detailed vibrational spectrum afforded by the heme group<sup>1</sup> in its varied protein settings. However, a completely satisfactory interpretational framework is not yet available despite a wealth of published data and despite the discovery of useful marker bands for the porphyrin core size, for the electron density of the frontier orbitals, and for the vibrations of specific axial ligands.<sup>2</sup> The spectra are rich and variable, and the effects of peripheral substituents and of distortions imposed by the protein are not easy to decipher. These effects, however, are of considerable interest with respect to heme protein structure and functions.

The first requirement for sound interpretation is a set of reliable vibrational assignments. There has been substantial progress in this direction through detailed isotopic studies coupled with normal coordinate analyses of model compounds, particularly of the nickel complexes of porphine, tetraphenylporphine (TPP),<sup>3</sup> octaethylporphyrin (OEP),<sup>4</sup> and etioporphyrin-I (EPI).<sup>5</sup> Using the framework developed in these model studies, we have recently assigned the very rich RR spectra of cytochrome c<sup>6</sup> using an enzymatic technique to replace the covalently bound endogenous heme with isotopically labeled

hemes. This study revealed strong RR signatures of protein-induced distortion of the heme.

In this work we assign the RR spectrum of myoglobin (Mb), again using several isotopic labels. Mb is a representation of the large class of proteins carrying noncovalently bound protoheme. The vinyl substituents in protoheme are conjugated with the porphyrin  $\pi$  system and have a strong influence on the RR spectra.<sup>7</sup> The nature of the influence has been a matter of debate, and an important objective of this work is to clarify this influence in the context of a protein-binding pocket. We are also able to gauge the role of the propionate substituents through propionate deuteration and have assigned a low-frequency band to a propionate bending mode. With assignments in hand, we have explored the effects of different oxidation and ligation states of Mb on the heme structure through changes in low-frequency RR spectra.

## Experimental Section

**Materials.** Horse heart myoglobin and natural abundance heme were purchased from Sigma, while other heme isotopomers were synthesized according to published procedures.<sup>8</sup> The propionate-labeled heme, designated as 6,7-di(d-D<sub>2</sub>)-heme, is also deuterated at the vinyl C<sub>b</sub> positions and at two methyl substituents: 2,4-di(b-D<sub>2</sub>)vinyl-1,3-bis-(deuteriomethyl)-6,7-di(d-D<sub>2</sub>).<sup>8b</sup>

**Preparation of Heme Isotopomer Reconstituted Myoglobins.** Apomyoglobin was prepared by Teale's butanone method<sup>9</sup> and dialyzed against three successive changes of buffers: 10 mM NaHCO<sub>3</sub> (4 h), 10 mM potassium phosphate (pH 7.0, 4 h), and finally 100 mM potassium phosphate (pH 7.0, 12 h). The precipitate of denatured protein was removed by centrifugation and discarded. The apomyoglobin, containing less than 5% heme, was used within 24 h. To prepare heme-labeled Mb, a slight excess of the appropriately labeled heme was dissolved in 0.1 N NaOH and added to the apomyoglobin solution with gentle stirring. Excess heme was removed by passage through a Sephadex G-25 column previously equilibrated with 0.1 M potassium phosphate buffer (pH 7.0). Deoxymyoglobin was prepared by addition of freshly prepared aqueous sodium dithionite in a NMR tube which had been flushed with argon. The CO adduct was formed by passing

\* Author to whom correspondence should be addressed.

<sup>†</sup> Princeton University.

<sup>‡</sup> University of California.

<sup>⊗</sup> Abstract published in *Advance ACS Abstracts*, November 15, 1996.

(1) For recent reviews on RR spectroscopy of heme proteins, see: (a) Abe, M. In *Advances in Spectroscopy*; Clark, R. J. H., Hester, R. E., Eds.; Wiley: New York, 1986; Vol. 13, 347–393. (b) Kitagawa, T.; Ozaki, Y. *Struct. Bonding* **1987**, *64*, 71–114. (c) Spiro, T. G.; Czernuszewicz, R. S.; Li, X.-Y. *Coord. Chem. Rev.* **1990**, *100*, 541–571. (d) Spiro, T. G.; Smulevich, G.; Su, C. *Biochemistry* **1990**, *29*, 4497–4508. (e) Procyk, A. D.; Bocian, D. F. *Annu. Rev. Phys. Chem.* **1992**, *43*, 465–496.

(2) Spiro, T. G., Ed. *Biological Applications of Raman Spectroscopy*; Wiley: New York; 1988, Vol. III.

(3) Li, X.-Y.; Czernuszewicz, R. S.; Kincaid, J. R.; Su, Y. O.; Spiro, T. G. *J. Phys. Chem.* **1990**, *94*, 31–47.

(4) (a) Abe, M.; Kitagawa, T.; Kyogoku, Y. *J. Chem. Phys.* **1978**, *69*, 4526–4534. (b) Li, X.-Y.; Czernuszewicz, R. S.; Kincaid, J. R.; Stein, P.; Spiro, T. G. *J. Phys. Chem.* **1990**, *94*, 47–61. (c) Li, X.-Y.; Czernuszewicz, R. S.; Kincaid, J. R.; Spiro, T. G. *J. Am. Chem. Soc.* **1989**, *111*, 7012–7023.

(5) Hu, S.; Mukherjee, A.; Piffat, C.; Mak, R. S. W.; Li, X.-Y.; Spiro, T. G. *Biospectroscopy* **1995**, *1*, 395–412.

(6) Hu, S.; Morris, I. K.; Singh, J. P.; Smith, K. M.; Spiro, T. G. *J. Am. Chem. Soc.* **1993**, *115*, 12446–12458.

(7) (a) Choi, S.; Spiro, T. G.; Langry, K. C.; Smith, K. M. *J. Am. Chem. Soc.* **1982**, *104*, 4337. (b) Choi, S.; Spiro, T. G.; Langry, K. C.; Smith, K. M.; Budd, L. D.; La Mar, G. N. *J. Am. Chem. Soc.* **1982**, *104*, 4345.

(8) (a) Kenner, G. W.; Smith, K. M.; Sutton, M. J. *Tetrahedron Lett.* **1973**, 1303–1306. (b) Budd, D. L.; La Mar, G. N.; Langry, K. C.; Smith, K. M.; Nayyir-Mazhir, R. *J. Am. Chem. Soc.* **1979**, *101*, 6091–6096. (c) Smith, K. M.; Morris, I. K. *J. Chem. Res., Synop.* **1988**, 16–17.

(9) Teale, F. W. J. *Biochim. Biophys. Acta* **1959**, *35*, 543.



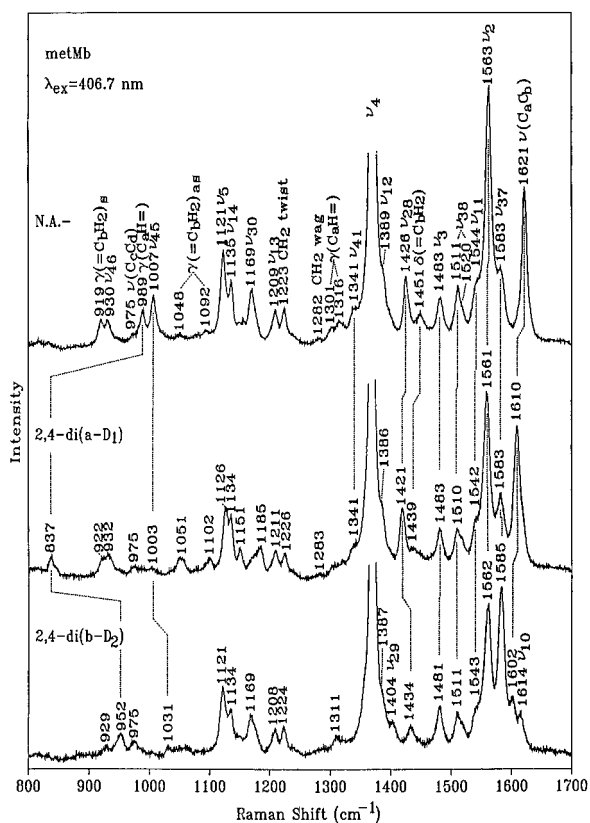


**Figure 3.** High-frequency resonance Raman spectra of metmyoglobin and its vinyl-deuterated isotopomers.

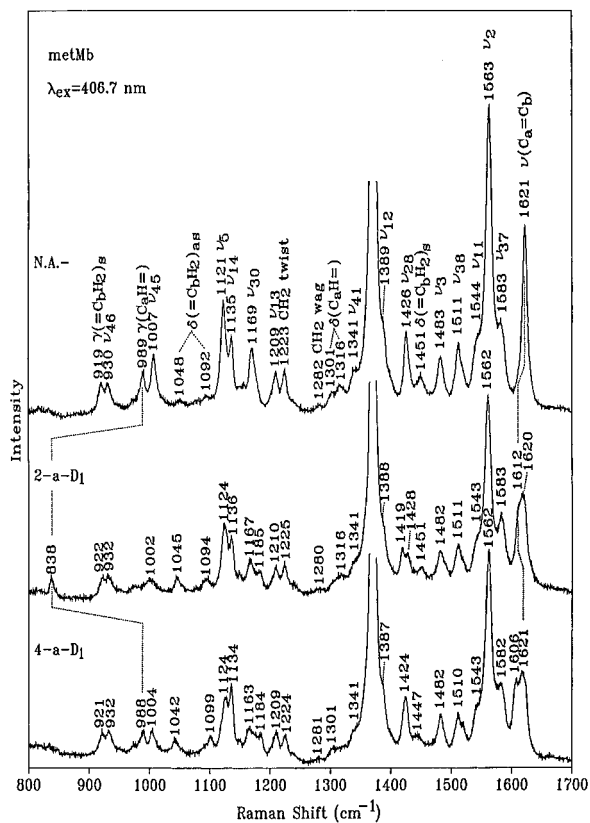


**Figure 4.** High-frequency resonance Raman spectra of metmyoglobin with selective labeling.

chosen to retain the NiOEP mode labels but have indicated modes which are localized to these bonds in Table 1 and 2.

**A. In-Plane Heme Modes. 1. Skeletal Mode Assignments.** Most assignments are readily made by extension of the

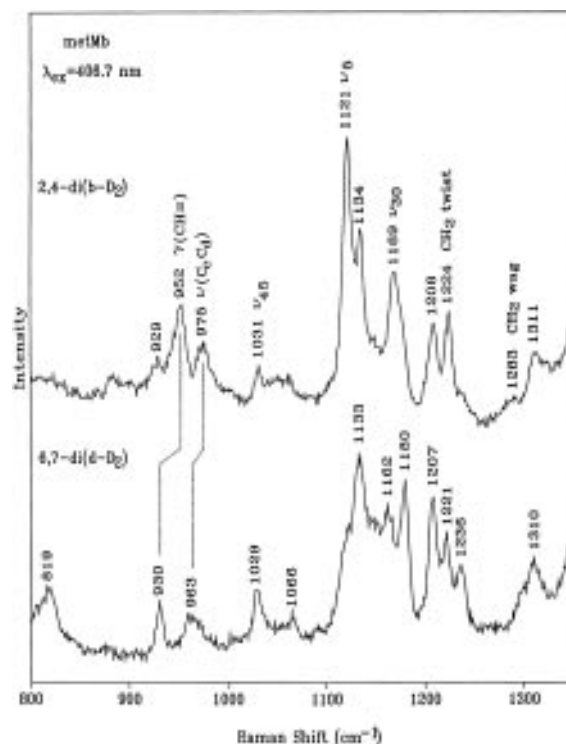


**Figure 5.** Effect of methyl and propionate labeling on the resonance Raman spectrum of metmyoglobin in the middle-frequency region.

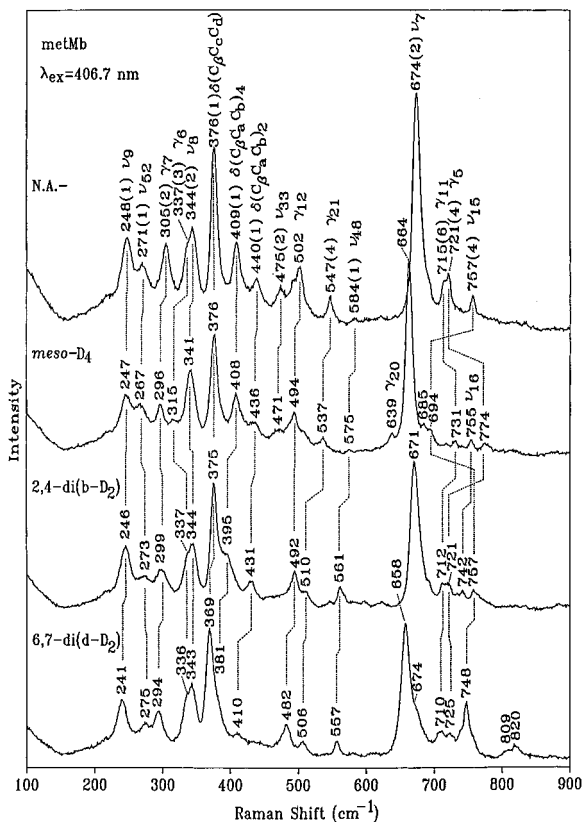


**Figure 6.** Low-frequency resonance Raman spectra of metmyoglobin and its isotopomers.

NiEPI<sup>5</sup> and cytochrome *c* assignments,<sup>6</sup> but we comment on features that are specific to protoheme. The highest-frequency C<sub>α</sub>C<sub>m</sub> asymmetrical stretching mode, ν<sub>10</sub>, was not observed for metMb, owing to its overlap with the strong vinyl C<sub>α</sub>=C<sub>β</sub> stretching band at 1621 cm<sup>-1</sup>, but it can be seen at 1614 cm<sup>-1</sup> in the RR spectrum of 2,4-di(b-d<sub>2</sub>) vinyl deuterated heme (Figure

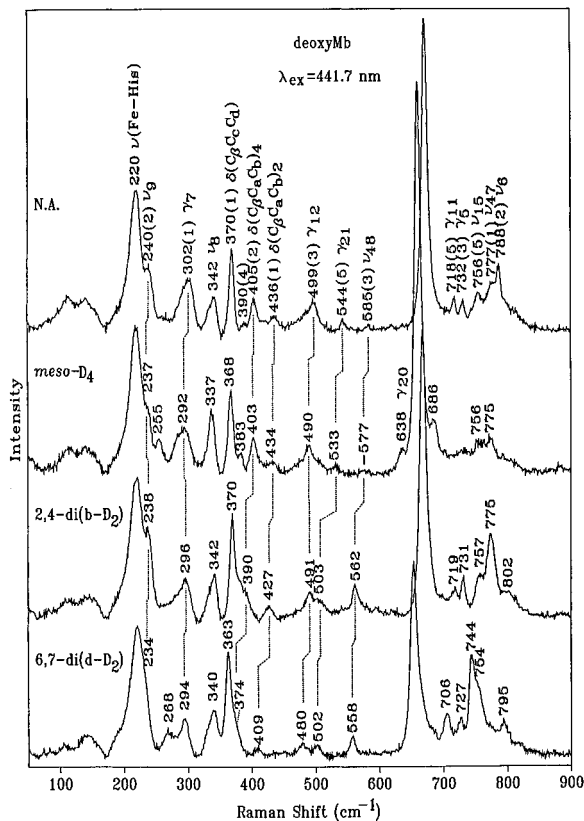


**Figure 7.** Low-frequency resonance Raman spectra of deoxymyoglobin and its isotopomers.

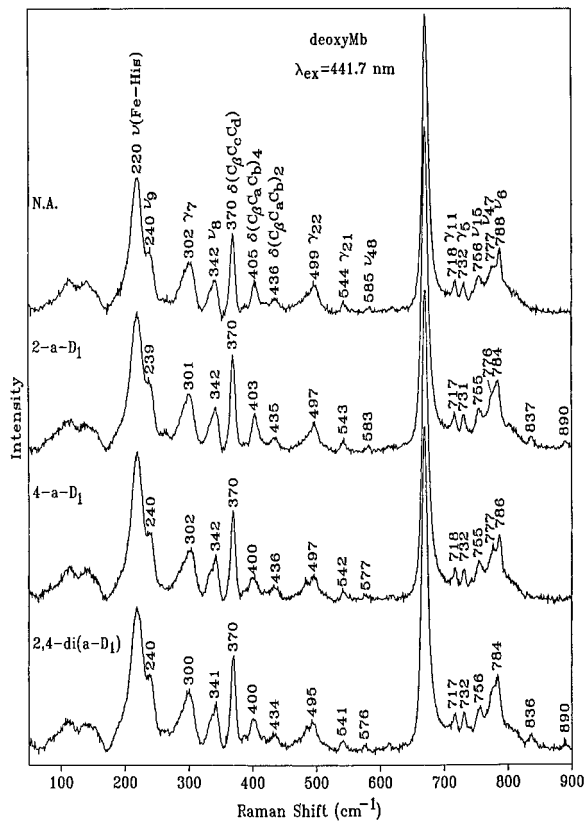


**Figure 8.** Low-frequency resonance Raman spectra of deoxymyoglobin and selective labeling.

3). This mode is shifted to  $1599\text{ cm}^{-1}$  upon deuteration of the heme *meso*-protons (Figure 2).

The very strong  $\nu_4$  band at  $1371\text{ cm}^{-1}$  has shoulders at  $1341$  and  $1389\text{ cm}^{-1}$ . We assign them to  $\nu_{41}$  and  $\nu_{12}$ , respectively.

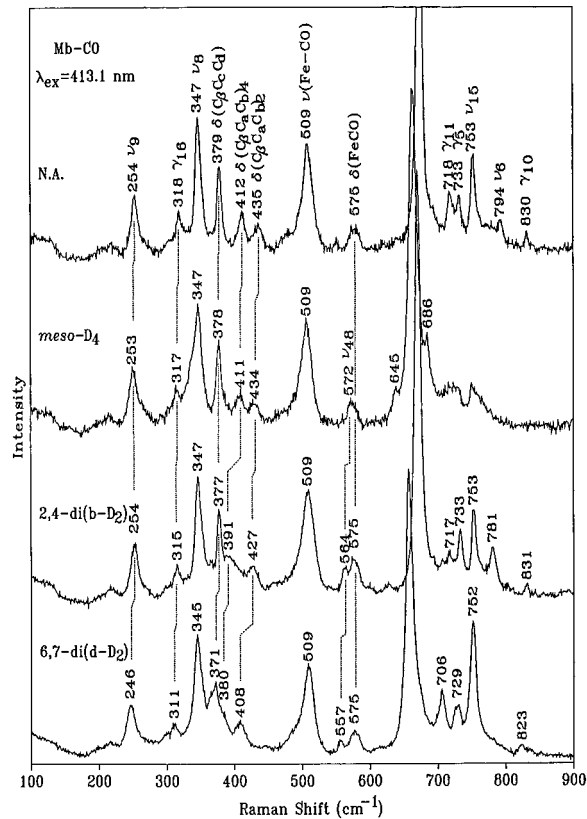


**Figure 9.** Low-frequency resonance Raman spectra of the carbon monoxide adduct of deoxymyoglobin and various isotopomers.

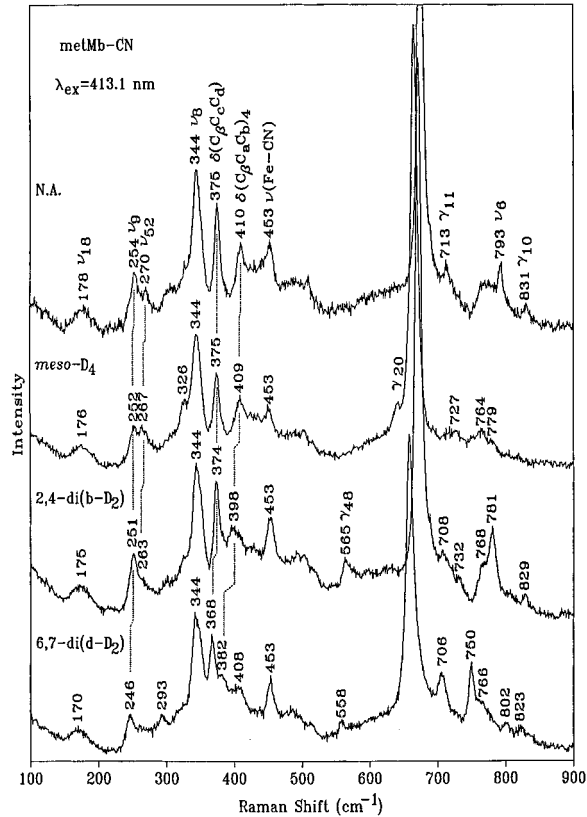


**Figure 10.** Low-frequency resonance Raman spectra of the cyanide adduct of metmyoglobin and various isotopomers.

These modes and  $\nu_4$  belong to the same local coordinate, the pyrrole half-ring symmetrical stretch, but with different phasing.<sup>4</sup> They are expected to show the same  $^{15}\text{N}$  shifts but drastically different *meso*-D<sub>4</sub> shifts, because contributions from C<sub>m</sub>-H

**Table 1.** Resonance Raman Frequencies and Their Normal Mode Assignments of Metmyoglobin and Its Isotopomers

N.A.	$\Delta(^{15}\text{N})$	<i>meso</i> -D <sub>4</sub>	2,4-di(a-D <sub>1</sub> )	2,4-di(b-D <sub>2</sub> )	2-a-D <sub>1</sub>	4-a-D <sub>1</sub>	6,7-di(d-D <sub>2</sub> )	assignment <sup>a</sup>
1621	0	1620	1610	1602	1612/1620	1606/1621	1600	$\nu(\text{C}_a=\text{C}_b)$
[1608] <sup>b</sup>		1599		1614	1583	1582	1614	$\nu_{10}$
1583	1	1579	1583	1583	1583	1582	1583	$\nu_{37}$
1563	0	1558	1561	1562	1562	1562	1559	$\nu_2$
1544	1	1532	1542	1543	1543	1543	1543	$\nu_{11}$
1521	1	1504	1518	1518	1520	1520		$\nu_{38}$
1511	1	1496	1510	1511	1511	1510	1509	$\nu_{38}$
1483	3	1476	1483	1481	1482	1482	1480	$\nu_3$
1451	2	1448	1439	952	1428/1451	1447		$\delta(=\text{C}_b\text{H}_2)_s$
1426	3	1420	1421	1434	1419	1424	1439	$\nu_{28}$
1402				1404			1403	$\nu_{29}$
1389	5	1325	1386	1387	1388	1387		$\nu_{12}$
1373	6	1372	1373	1373	1373	1373	1373	$\nu_4$
1341	3		1341		1341	1341		$\nu_{41}$
1316	1		975	1311	1316	974	1310	$\delta(\text{C}_a\text{H}=\text{C}_b)_4$
1301	0	1301	975	1289	974	1302		$\delta(\text{C}_a\text{H}=\text{C}_b)_2$
1282	2	1282	1283		1280	1281		
1223	2	1224	1226	1224	1225	1224		
1209	3	951	1211	1208	1210	1209		$\nu_{13}$
1169	6	1170		1169	1167	1163		$\nu_{30}$
1135	13	1145	1134	1134	1136	1134		$\nu_{14}$
1121	8	1120	1126	1121	1124	1124		$\nu_5$ (C <sub><math>\beta</math></sub> -methyl stretch)
1092	5		1102		1094	1099		$\delta(=\text{C}_b\text{H}_2)_{as}$
1048	0		1051		1045	1042		$\delta(=\text{C}_b\text{H}_2)_{as}$
1007	2	1010	1003	1031	1002	1004		$\nu_{45}$ (C <sub><math>\beta</math></sub> -vinyl stretch)
989	0	989	837	975	838	988		$\gamma(\text{C}_a\text{H}=\text{C}_b)$
930	6		932	929		932		$\nu_{46}$
919	1		922		922	921		$\gamma(=\text{C}_b\text{H}_2)_s$
757	4	694	757	757	757	757	748	$\nu_{15}$
721	4	774	720	721	721	721	725	$\gamma_5$
715	6	731	714	712	714	715	710	$\gamma_{11}$
674	1	664	673	671	674	674	658	$\nu_7$
584	1	575	576	561	584		557	$\nu_{48}$
547	4	537	545	547	546	546		$\gamma_{21}$
502	0	494	495	492	500	495	482	$\gamma_{12}$
475	2	471	467		468	471		$\nu_{33}$
440	1	436	437	431	439	438	410	$\delta(\text{C}_\beta\text{C}_a\text{C}_b)_2 + \delta(\text{C}_\beta \text{Me})$
409	1	408	407	395	409	407		$\delta(\text{C}_\beta\text{C}_a\text{C}_b)_4 + \delta(\text{C}_\beta \text{Me})$
376	1	376	376	375	376	376	369	$\delta(\text{C}_\beta\text{C}_c\text{C}_d)$
344	2	341	344	344	344	344	343	$\nu_8$
337	3	315	337	337	337	337	336	$\gamma_6$
305	2	296	302	299	303	304	294	$\gamma_7$
271	1	267	269	273	271	270	275	$\nu_{52}$
248	1	247	247	246	248	248	241	$\nu_9$

<sup>a</sup> Mode compositions are expected to be similar to those of NiOEP, which are given in ref 4b. <sup>b</sup> This band is observed by the strong  $\nu(\text{C}_a=\text{C}_b)$  band, but is readily located with excitation at wavelengths in the Q-region (see e.g., ref 22).

bending are forbidden in A<sub>1g</sub> symmetry ( $\nu_4$ ) but allowed in B<sub>1g</sub> ( $\nu_{12}$ ) and E<sub>u</sub> ( $\nu_{41}$ ) symmetry. All these bands shift 3–5 cm<sup>-1</sup> in the <sup>15</sup>N spectra, and  $\nu_4$  is insensitive to *meso*-D<sub>4</sub> substitution as expected. On the other hand,  $\nu_{12}$  moves from 1389 to 1325 cm<sup>-1</sup> in the *meso*-D<sub>4</sub> spectrum just as it does in NiEPI.<sup>5</sup> Because of its overlap with  $\nu_4$ ,  $\nu_{12}$  had only been detected for NiOEP upon *meso*-D<sub>4</sub> substitution, but its position in the natural abundance spectrum was revealed by FT-Raman spectroscopy of NiEPI, with 1064-nm preresonant excitation.<sup>5</sup>

The 1341-cm<sup>-1</sup> band was previously assigned by Choi et al. to one of the two vinyl =C<sub>b</sub>H<sub>2</sub> scissor modes on the basis of an apparent 5-cm<sup>-1</sup> 2,4-di(a-D<sub>1</sub>) shift.<sup>7</sup> This shift, however, is not reproduced in the present spectrum (Figure 3), which is better resolved than the previous spectra. Upon *meso*-D<sub>4</sub> substitution, the 1341-cm<sup>-1</sup> band shifts down about 7 cm<sup>-1</sup>, appearing as a shoulder on the 1325-cm<sup>-1</sup>  $\nu_{12}$  band. The shift is that expected for  $\nu_{41}$ , which is calculated at 1346 cm<sup>-1</sup> in NiOEP, with 5- and 4-cm<sup>-1</sup> <sup>15</sup>N and *meso*-D<sub>4</sub> shifts.

The 1000–1150-cm<sup>-1</sup> region contains bands that are allocated to stretching of the porphyrin–substituent bands (C <sub>$\beta$</sub> –C<sub>1</sub> Table 2). As noted above, assignment of these bands to NiOEP-derived modes is arbitrary, because of the inequivalence of the C <sub>$\beta$</sub> –C<sub>1</sub> bonds. For example, the 1007-cm<sup>-1</sup> band is assigned

to  $\nu_{45}$  because of its match to the frequency calculated for NiOEP (996 cm<sup>-1</sup>) and observed for NiEPI (990 cm<sup>-1</sup>). However, it is actually a superposition of porphyrin–vinyl stretches, as evidenced by its loss in intensity upon C<sub>a</sub>-deuteration of either the 2- or 4-vinyl groups (Figure 4) and by its disappearance when both vinyl groups are deuterated (Figure 3). Choi et al.<sup>7</sup> had assigned the 1121-cm<sup>-1</sup> band, now allocated to  $\nu_5$ , to porphyrin–vinyl stretching based on its 5-cm<sup>-1</sup> upshift upon C<sub>a</sub> deuteration (Figure 3). However, this band undergoes a 12-cm<sup>-1</sup> upshift in the 6,7-di(d-D<sub>2</sub>) isotopomer (Figure 5) and probably involves porphyrin–methyl stretching; this coordinate would be depressed in frequency by interaction with the –CH<sub>3</sub> umbrella coordinate (~1365 cm<sup>-1</sup>), but raised in frequency when the interaction is relieved by deuteration of the 1- and 3-methyl groups. A similar effect was observed in NiEPI<sup>5</sup> in which  $\nu_5$  shifted from 1137 to 1152 cm<sup>-1</sup> upon perdeuteration of the methyl groups. We note also that  $\nu_{30}$ , allocated to a pyrrole half-ring coordinate (Table 2), likewise shifted up 14 cm<sup>-1</sup> upon methyl perdeuteration in NiEPI,<sup>5</sup> implying substantial C <sub>$\beta$</sub> –C<sub>1</sub> involvement, and similarly the 1169-cm<sup>-1</sup> band assigned to  $\nu_{30}$  in Mb shifts up to 1180 cm<sup>-1</sup> in the 6,7-di(d-D<sub>2</sub>) isotopomer (Figure 5).

Below 600 cm<sup>-1</sup> (Figure 6), two A<sub>1g</sub> modes  $\nu_8$  and  $\nu_9$  are

**Table 2.** Allocation of the Observed In-plane Skeletal Frequencies of metmyoglobin to the Local Coordinates<sup>a</sup>

local coordinate	A <sub>1g</sub>	B <sub>1g</sub>	A <sub>2g</sub>	B <sub>2g</sub>	E <sub>u</sub>
$\nu(\text{C}_m\text{H})$	$\nu_1$ [3041]			$\nu_{27}$ [3041]	$\nu_{36}$ [3040]
$\nu(\text{C}_\alpha\text{C}_m)_{\text{asym}}$		$\nu_{10}$ 1614 1655	$\nu_{19}$ 1603		$\nu_{37}$ 1583 [1602]
$\nu(\text{C}_\beta\text{C}_\beta)$	$\nu_2$ 1563 1602	$\nu_{11}$ 1544 1577			$\nu_{38}$ 1511/1521 1604
$\nu(\text{C}_\alpha\text{C}_m)_{\text{sym}}$	$\nu_3$ 1483 1520			$\nu_{28}$ 1426 1483	$\nu_{39}$ 1501
$\nu(\text{pyr quarter-ring})$			$\nu_{20}$ 1393	$\nu_{29}$ 1404 1407	$\nu_{40}$ 1396
$\nu(\text{pyr half-ring})_{\text{sym}}$	$\nu_4$ 1373 1384	$\nu_{12}$ 1389 1387 <sup>b</sup>			$\nu_{41}$ 1341 [1346]
$\delta(\text{C}_m\text{H})$		$\nu_{13}$ 1209 1220	$\nu_{21}$ 1307		$\nu_{42}$ 1231
$\nu(\text{C}_\beta\text{C}_1)_{\text{sym}}$	$\nu_5$ 1121 <sup>c</sup> 1138	$\nu_{14}$ 1135 1131			$\nu_{44}$ 1153
$\nu(\text{pyr half-ring})_{\text{asym}}$			$\nu_{22}$ 1121	$\nu_{30}$ 1169 1159	$\nu_{43}$ 1133
$\nu(\text{C}_\beta\text{C}_1)_{\text{asym}}$			$\nu_{23}$ 1058	$\nu_{31}$ 1015	$\nu_{45}$ 1007 <sup>d</sup> 996
$\delta(\text{pyr deform})_{\text{asym}}$			$\nu_{24}$ 597	$\nu_{32}$ 938	$\nu_{46}$ 930 927
$\nu(\text{pyr breathing})$	$\nu_6$ 804	$\nu_{15}$ 757 751			$\nu_{47}$ 766
$\delta(\text{pyr deform})_{\text{sym}}$	$\nu_7$ 674 674	$\nu_{16}$ 746			$\nu_{48}$ 584 605
$\delta(\text{pyr rot.})$			$\nu_{25}$ 551	$\nu_{33}$ 475 493	$\nu_{49}$ 544
$\nu(\text{M-N})$	$\nu_8$ 344 361/343	$\nu_{18}$ 168			$\nu_{50}$ [358]
$\delta(\text{C}_\beta-\text{C}_1)_{\text{asym}}$			$\nu_{26}$ [243]	$\nu_{34}$ 197	$\nu_{51}$ 328
$\delta(\text{C}_\beta\text{C}_1)_{\text{sym}}$	$\nu_9$ 248 <sup>e</sup> 263/274	$\nu_{17}$ 305			$\nu_{52}$ 271 <sup>e</sup> 263
$\delta(\text{pyr transl})$				$\nu_{35}$ 144	$\nu_{53}$ 212

<sup>a</sup> The italicized values are those of NiOEP.<sup>4b</sup> The bracketed values are the calculated frequencies for which the experimental values are not available. <sup>b</sup> Detected for NiEPI.<sup>5</sup> <sup>c</sup> Primarily  $\nu(\text{C}_\beta-\text{methyl})$ . <sup>d</sup> Primarily  $\nu(\text{C}_\beta-\text{vinyl})$ . <sup>e</sup> Coupled  $\delta(\text{C}_\beta-\text{propionate})$  and  $\delta(\text{C}_\beta-\text{methyl})$ .

**Table 3.** Allocation of the Observed Out-of-Plane Modes of Metmyoglobin to the Local Coordinates<sup>a</sup>

local coordinates	A <sub>1u</sub>	A <sub>2u</sub>	B <sub>1u</sub>	B <sub>2u</sub>	E <sub>g</sub>
$\gamma(\text{C}_m\text{H})$		$\gamma_4$ 844	$\gamma_{10}$ 830 <sup>b</sup> 853		$\gamma_{19}$ 841
Pyr fold <sub>asym</sub>	$\gamma_1$ 750		$\gamma_{11}$ 715 729		$\gamma_{20}$ <sup>c</sup> [713]
Pyr fold <sub>sym</sub>		$\gamma_5$ 721 739		$\gamma_{15}$ 704	$\gamma_{21}$ 547 656
Pyr swivel	$\gamma_2$ [346]		$\gamma_{12}$ 502 612		$\gamma_{22}$ 492
Pyr tilt		$\gamma_6$ 337 360		$\gamma_{16}$ 318 <sup>d</sup> 270	$\gamma_{23}$ 254
$\gamma(\text{C}_\alpha\text{C}_m)$		$\gamma_7$ 305 [284]	$\gamma_{13}$ [130]		$\gamma_{24}$ 230
$\gamma(\text{C}_\beta\text{C}_1)_{\text{sym}}$		$\gamma_8$ [108]		$\gamma_{17}$ 127	$\gamma_{25}$ [91]
$\gamma(\text{C}_\beta\text{C}_1)_{\text{asym}}$	$\gamma_3$ [74]		$\gamma_{14}$ [44]		$\gamma_{26}$ [63]
Pyr transl				$\gamma_{18}$ [30]	
$\gamma(\text{NiN})$		$\gamma_9$ [32]			

<sup>a</sup> The italicized values are those of NiOEP. The bracketed values are the calculated frequencies for which the experimental values are not available. <sup>b</sup> Seen in MbCO and metMbCN. <sup>c</sup> Seen at 639 cm<sup>-1</sup> upon *meso*-D<sub>4</sub> substitution. <sup>d</sup> Seen in MbCO.

expected and were previously assigned at 344 and 271 cm<sup>-1</sup>.<sup>7</sup> The  $\nu_8$  assignment is confirmed by the 2-cm<sup>-1</sup> <sup>15</sup>N and 3-cm<sup>-1</sup> *meso*-D<sub>4</sub> shifts of the 344-cm<sup>-1</sup> band, but  $\nu_9$  is reassigned to the 248-cm<sup>-1</sup> band because of the expected insensitivity of  $\nu_9$  to *meso*-deuteration.<sup>4</sup> The 4-cm<sup>-1</sup> *meso*-D<sub>4</sub> shift of the 271-

cm<sup>-1</sup> band suggests assignment to  $\nu_{52}$ , which is observed at 263 cm<sup>-1</sup> in NiOEP, with a 3-cm<sup>-1</sup> *meso*-D<sub>4</sub> shift. Both  $\nu_9$  and  $\nu_{52}$  are allocated to porphyrin-substituent bending coordinates ( $\text{C}_\beta-\text{C}_1$ , Table 2), but their sensitivity to the available isotopomers is slight (Figure 6). The biggest shifts are seen in the 6,7-di(d-D<sub>2</sub>) spectra, -7 cm<sup>-1</sup> for  $\nu_9$  and +4 cm<sup>-1</sup> for  $\nu_{52}$ , suggesting that the  $\text{C}_\beta$ -propionate bends are involved along with the  $\text{C}_\beta$ -methyl bends of the adjacent 5- and 8-methyl groups (Figure 1). If the 1- and 3-methyl groups were major contributions, then larger shifts would have been expected, since in NiOEP,  $\nu_9$  shifts down 30 cm<sup>-1</sup> when the ethyl C<sub>1</sub> atoms are deuterated.

**2. Vinyl Influences.** Vinyl groups are known to induce Raman activity in E<sub>u</sub> modes and to remove their degeneracy.<sup>7</sup> These effects are confirmed in the spectra of metMb. In the high-frequency region (1450–1700 cm<sup>-1</sup>), both  $\nu_{37}$  and  $\nu_{38}$  are seen with significant intensity (Figure 2). Moreover,  $\nu_{38}$  is split into two components at 1511 and 1521 cm<sup>-1</sup>. These two bands become well-resolved at 1496 and 1504 cm<sup>-1</sup> in the spectrum for the *meso*-D<sub>4</sub> isotopomer. In this frequency region, the modes are mixtures of  $\text{C}_\beta-\text{C}_\beta$  and  $\text{C}_\alpha-\text{C}_m$  coordinates, but the much larger *meso*-D<sub>4</sub> shift of  $\nu_{38}$  (16 cm<sup>-1</sup>) than that of  $\nu_{37}$  (4 cm<sup>-1</sup>) implies predominant  $\text{C}_\beta\text{C}_\beta$  character for the former and  $\text{C}_\alpha\text{C}_m$  character for the latter. As discussed in the preceding section,  $\nu_{41}$  is now assigned to the 1341-cm<sup>-1</sup> band; we note that this band is polarized with Soret excitation, but has been reported to be anomalously polarized when excited in the vicinity of the Q-bands.<sup>11</sup> This behavior suggests that the two E<sub>u</sub> components are superimposed and have different polarization, one being enhanced in resonance with the Soret band and the other in resonance with the Q-bands. Additional E<sub>u</sub> modes are assigned at 1007 ( $\nu_{45}$ ), 930 ( $\nu_{46}$ ), 584 ( $\nu_{48}$ ), and 252 ( $\nu_{52}$ ) cm<sup>-1</sup> on the basis of their frequency and isotopic correspondences with E<sub>u</sub> modes of NiOEP<sup>4</sup> and NiEPI.<sup>5</sup>

Vinyl coordinates are mixed into some of the skeletal modes. The  $\nu_2$  (1563 cm<sup>-1</sup>) and  $\nu_{11}$  (1544 cm<sup>-1</sup>) modes are shifted down 2 cm<sup>-1</sup> for the 2,4-di(a-D<sub>1</sub>) isotopomer (Figure 3). More pronounced mixing is observed for  $\nu_{28}$ , which shifts from 1426 down to 1421 cm<sup>-1</sup> for C<sub>a</sub> deuteration and up to 1434 cm<sup>-1</sup> for C<sub>b</sub> deuteration. This effect is due to interaction with the neighboring vinyl =CH<sub>2</sub> scissor mode, 1451 cm<sup>-1</sup>, which shift down to 1439 cm<sup>-1</sup> upon C<sub>a</sub> deuteration (see next section). When C<sub>b</sub> is deuterated, the scissor mode shifts out of the region, thereby relieving the interaction and causing  $\nu_{28}$  to shift up. A frequency upshift is also seen for  $\nu_{29}$  (1401 cm<sup>-1</sup>), which appears as a shoulder on the strong  $\nu_4$  band, but becomes a distinct band at 1404 cm<sup>-1</sup> upon C<sub>b</sub> deuteration (Figure 3).

The vinyl groups also induce a significant change in the normal mode composition of  $\nu_2$  and  $\nu_{11}$ . These two modes are calculated to be nearly pure  $\text{C}_\beta-\text{C}_\beta$  stretching vibrations. They show no *meso*-D<sub>4</sub> sensitivity in NiOEP,<sup>4</sup> NiEPI,<sup>5</sup> or cytochrome *c*,<sup>6</sup> but shift down 5 and 11 cm<sup>-1</sup> in metMb. This sensitivity implies a significant contribution of the  $\text{C}_\alpha-\text{C}_m$  coordinate to the modes. The coordinate mixing cannot be ascribed to symmetry lowering alone, in view of the NiEPI and cytochrome *c* spectra,<sup>6</sup> but must arise as a specific effect of the vinyl substituents.

**B. Substituent Modes.** Protoheme possesses three sets of peripheral substituents, the vinyl, propionate, and methyl groups (Figure 1). In addition to the porphyrin-substituent stretches and bends described above, the internal vibrations of these groups are expected to exhibit RR activity inasmuch as ethyl and methyl vibrations have been shown to be enhanced in the RR spectra of NiOEP<sup>4</sup> and NiEPI.<sup>5</sup>

(11) Spiro, T. G.; Strekas, T. C. *Proc. Natl. Acad. Sci. U.S.A.* **1972**, *69*, 2622–2626.

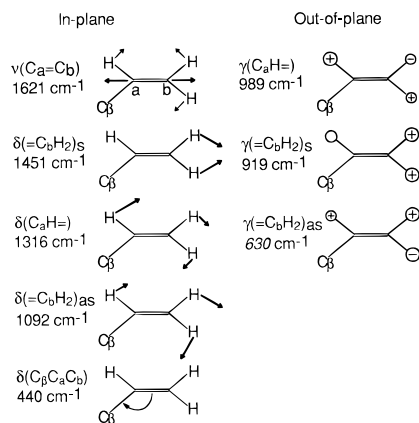


**Figure 11.** Diagram of the vinyl vibrations with frequencies assigned from metMb spectra. The  $630\text{-cm}^{-1}$   $\gamma(=\text{C}_b\text{H}_2)_{as}$  is not seen. The  $410\text{-cm}^{-1}$   $\delta(\text{C}_\beta\text{C}_a\text{C}_b)$  mode is formally included among the porphyrin skeletal modes ( $\delta\text{C}_\beta\text{-C}_1$ ).

**1. Vinyl Modes.** Although most of the vinyl modes were previously identified in the RR spectrum and assigned via deuteration,<sup>7</sup> some of these assignments are revisited in connection with the available *meso*-D<sub>4</sub> and <sup>15</sup>N shifts. Figure 11 summarizes the observed frequencies of vinyl modes for metMb, along with a schematic description of their eigenvectors. Some notable aspects are discussed here with a view toward clarifying controversies in the literature.

$\nu(\text{C}_a=\text{C}_b)$ . The two  $\nu(\text{C}_a=\text{C}_b)$  modes coincide in a single band at  $1621\text{ cm}^{-1}$ . They are, however, revealed by selective labeling of the vinyl groups. When either group is deuterated at C<sub>a</sub>, a split band is observed (Figure 4) with one component at  $1621\text{ cm}^{-1}$  and the other at a lower frequency. However, the position of the lower component is different,  $1612\text{ cm}^{-1}$  for 2-a-D<sub>1</sub> heme but  $1606\text{ cm}^{-1}$  for 4-a-D<sub>1</sub> heme. The differing isotope shifts imply different mode compositions, even though the frequencies are the same in unlabeled protein.

$\delta(=\text{C}_b\text{H}_2)_s$ . The vinyl  $=\text{CH}_2$  scissor mode is reassigned to a spectral feature at  $1451\text{ cm}^{-1}$ . (It was earlier assigned to the  $1426\text{-cm}^{-1}$  band, now reassigned to  $\nu_{28}$ , see above.) The  $1451\text{-cm}^{-1}$  band shifts to  $1439\text{ cm}^{-1}$  and disappears for 2,4-di(a-D<sub>1</sub>) and 2,4-di(b-D<sub>2</sub>) isotopomers, respectively. The  $\delta(=\text{CH}_2)_s$  and  $\nu_{28}$  modes are strongly coupled, as discussed above.

Inequivalent vinyl modes are again revealed by selective labeling. C<sub>a</sub> deuteration of the 4-vinyl group (Figure 4) broadens the  $1451\text{-cm}^{-1}$  band and shifts its center to  $1447\text{ cm}^{-1}$ ;  $\nu_{28}$  is shifted only  $2\text{ cm}^{-1}$ . However, C<sub>a</sub> deuteration of the 2-vinyl group clearly splits the  $\delta(=\text{C}_b\text{H}_2)_s$  band, with one component shifted down to  $1428\text{ cm}^{-1}$ ;  $\nu_{28}$  is now shifted  $7\text{ cm}^{-1}$ . Intriguingly, 2-vinyl deuteration has a greater effect than that of deuteration of both vinyl groups (Figure 3), while 4-vinyl deuteration has a much smaller effect.

The assignment of both  $\delta(=\text{C}_b\text{H}_2)_s$  modes to the  $1451\text{-cm}^{-1}$  band supplants the earlier assignment of one of these modes to the  $1341\text{-cm}^{-1}$  band (now reassigned to  $\nu_{41}$ , see above), an assignment that had been questioned by Kitagawa and co-workers<sup>12</sup> on the basis of a model normal mode calculation.

$\delta(\text{C}_a\text{H}=\text{C})$ . The in-plane C–H bending mode was previously identified at  $1305\text{ cm}^{-1}$  for NiPPIX and at  $1314\text{ cm}^{-1}$  for fluorometMb.<sup>7</sup> We detected two well-resolved spectral features at  $1301$  and  $1316\text{ cm}^{-1}$  that can be assigned to  $\delta(\text{C}_a\text{H}=\text{C})$ . These two features disappear in the spectra of 2,4-di(a-D<sub>1</sub>) and collapse into a single band at  $1311\text{ cm}^{-1}$  for 2,4-di(b-D<sub>2</sub>) heme. Furthermore, we are able to assign the  $1301\text{-}$  and  $1316\text{-cm}^{-1}$

bands to the 2- and 4-vinyl group, respectively, because of their selective disappearance in the 2-a-D<sub>1</sub> and 4-a-D<sub>1</sub> spectrum. Thus the two vinyl groups have distinctly different frequencies for this mode.

$\delta(=\text{C}_b\text{H}_2)_{as}$ . The vinyl CH<sub>2</sub> rocking modes are assigned to a pair of weak features at  $1048$  and  $1092\text{ cm}^{-1}$ ; the latter is close to the  $1089\text{-cm}^{-1}$  RR band previously observed for NiPPIX.<sup>7</sup> These two bands shift slightly and intensify for 2,4-di(a-D<sub>1</sub>) heme, but disappear for 2,4-di(b-D<sub>2</sub>). The C<sub>a</sub> deuteration shifts are too small to distinguish the vinyl groups by selective labeling.

$\gamma(\text{C}_a\text{H}=\text{C})$ . The out-of-plane C<sub>a</sub>H= wag is assigned to a spectral feature at  $989\text{ cm}^{-1}$ , which disappears for both 2,4-di(a-D<sub>1</sub>) and 2,4-di(b-D<sub>2</sub>) hemes. The previously allocated band at  $1007\text{ cm}^{-1}$  is reassigned to  $\nu_{45}$  on the basis of its expected *meso*-D<sub>4</sub> and <sup>15</sup>N shifts. Interestingly, the  $989\text{-cm}^{-1}$  band seems to derive its intensity solely from the 2-vinyl group. The spectrum of 2-a-D<sub>1</sub> heme exhibits complete loss of the  $989\text{-cm}^{-1}$  band and the occurrence of a new feature at  $838\text{ cm}^{-1}$ , assignable to  $\gamma(\text{CD}=\text{C})$ , while the  $989\text{-cm}^{-1}$  intensity is unaffected in the spectrum of 4-a-D<sub>1</sub> heme and no new feature is discernible in the  $800\text{--}1000\text{-cm}^{-1}$  spectral region.

$\gamma(=\text{C}_b\text{H}_2)_s$ . The symmetric  $=\text{CH}_2$  wag is located at  $919\text{ cm}^{-1}$  for metMb. It disappears for 2,4-di(b-D<sub>2</sub>) heme and shifts up to  $922\text{ cm}^{-1}$  upon C<sub>a</sub> deuteration in either vinyl group (Figure 4). This mode was assigned to the  $903\text{-cm}^{-1}$  IR band for NiPPIX<sup>7</sup> and has not been detected in other RR spectra. It seems to derive its intensity from the nearby  $\nu_{46}$  ( $930\text{ cm}^{-1}$ ); the  $919\text{-cm}^{-1}$  band vanishes when  $\nu_{46}$  loses its intensity in *meso*-D<sub>4</sub> heme (Figure 2).

$\delta(\text{C}_\beta\text{C}_a\text{C}_b)$ . Two vinyl bending modes are assigned, at  $405\text{--}412$  and  $435\text{--}440\text{ cm}^{-1}$ , on the basis of their  $8\text{--}15\text{-cm}^{-1}$  C<sub>b</sub>D<sub>2</sub> downshifts (Figures 6, 8, and 9). Deuteration at C<sub>a</sub> produces only slight shifts (Figure 7) because C<sub>a</sub> is the central atom of the bending coordinate and its motion is small. However, selective labeling shows these shifts to be localized to the 4-vinyl group for the lower frequency band and the 2-vinyl group for the higher frequency band (Figure 7). Thus the two vinyl groups have quite different frequencies for the bending mode. Some of this difference is associated with the substantial coupling to the 1- and 3-methyl group coordinates that are evident in the 6,7-di(d-D<sub>2</sub>) spectra (Figures 6, 8, and 9). Relative to the 2,4-di(b-D<sub>2</sub>) spectra (the vinyl C<sub>b</sub> atoms are deuterated in both isotopomers), the 6,7-di(d-D<sub>2</sub>) shifts are  $\sim 12\text{ cm}^{-1}$  for  $\delta(\text{C}_\beta\text{C}_a\text{C}_b)_4$  and  $\sim 20\text{ cm}^{-1}$  for  $\delta(\text{C}_\beta\text{C}_a\text{C}_b)_2$ . Thus these modes should really be viewed as coupled vinyl and methyl bends on the two vinyl-bearing pyrrole rings (Figure 1).

We note that Gersonde et al.<sup>13</sup> assigned vinyl bending modes at  $412$  and  $591\text{ cm}^{-1}$  in a vinyl-labeled monomeric insect hemoglobin. The latter frequency corresponds to the  $584\text{-cm}^{-1}$  band in Mb, which we assign to the skeletal mode  $\nu_{48}$ , on the basis of its substantial <sup>15</sup>N and *meso*-D<sub>4</sub> shifts. We confirm, however, that vinyl deuteration shifts are large,  $9\text{ cm}^{-1}$  for C<sub>a</sub>–D (Figure 7) and  $23\text{ cm}^{-1}$  for C<sub>b</sub>–D<sub>2</sub> (Figures 6 and 8), implying strong coupling with vinyl bending. Interestingly the effect appears to be localized to the 4-vinyl group, as judged by selective labeling (Figure 7).

**2. Propionate Modes.** The propionate groups at the 6,7 positions resemble the ethyl groups in NiOEP. In view of the significant RR activity of these aliphatic groups in the RR spectra of NiOEP,<sup>4</sup> the propionate modes are expected to show up in the Mb spectra. The propionate assignments were suggested for cytochrome *c* on the basis of small isotope shifts

(12) Lee, H.; Kitagawa, T.; Abe, M.; Pandey, P. K.; Leung, H.-K.; Smith, K. M. *J. Mol. Struct.* **1986**, *146*, 329–347.

(13) Gersonde, K.; Yu, N.-T.; Lin, S. H.; Smith, K. M.; Parish, D. W. *Biochemistry* **1989**, *28*, 8197–8201.

and by analogy to the ethyl modes of NiOEP.<sup>4</sup> They are confirmed for Mb by comparing the spectra of 2,4-di(*b*-D<sub>2</sub>) and 6,7-di(*d*-D<sub>2</sub>) (Figure 5).

**Methylene Deformations.** Expected CH<sub>2</sub> bending modes include the scissors (~1440 cm<sup>-1</sup>), wag (~1300 cm<sup>-1</sup>), twist (~1250 cm<sup>-1</sup>), and rock (~750 cm<sup>-1</sup>). No RR candidates are found for the first two of these, but the 1223- and 1282-cm<sup>-1</sup> bands can be assigned to methylene twist and wag deformations on the basis of the propionate labeling (Figure 5).

$\nu(\text{C}_c-\text{C}_d)$ . In cytochrome *c*, a pair of bands at ~970 cm<sup>-1</sup> was assigned to C<sub>c</sub>-C<sub>d</sub> stretching. A weak feature is also observed in Mb at 975 cm<sup>-1</sup> (Figure 5), which is unaffected by isotope substitution except when the propionates are labeled.

$\delta(\text{C}_\beta\text{C}_c\text{C}_d)$ . Particular interest attaches to the 376-cm<sup>-1</sup> band, which is the strongest band below 600 cm<sup>-1</sup> for metMb (Figure 6). This band is assigned to the porphyrin-propionate bending because its frequency is invariant for all isotopomers except 6,7-di(*d*-D<sub>2</sub>), for which it shifts down 6 cm<sup>-1</sup>. This modest shift is consistent with the effect of deuteration at the second propionate methylene group (C<sub>d</sub>) on the bending frequency. This band is at the same frequency in metMb-CN<sup>-</sup> (Figure 8) and at a slightly higher frequency in MbCO (379 cm<sup>-1</sup>, Figure 9), but at a distinctly lower frequency in deoxyMb (Figure 7). In metMb and deoxyMb, its intensity is higher than that of  $\nu_8$ , normally the strongest low-frequency band in metalloporphyrin spectra, but in metMb-CN<sup>-</sup> and MbCO,  $\nu_8$  is stronger. Bands in this region have also been identified in cytochrome *c* and CCP and have moderate intensities. The frequency and intensity variations may be related to conformational changes of the propionate substituents.

**3. Ring-Adjacent Methyl Groups.** Although some methyl modes (rocking mode at ~1060 cm<sup>-1</sup> and umbrella mode at 1362 cm<sup>-1</sup>) were identified in the spectra of cytochrome *c*,<sup>6</sup> no candidate band is seen in the 406-nm excitation spectra of Mb derivatives.

**C. Out-of-Plane Vibrations.** In the low-frequency (100–900-cm<sup>-1</sup>) region, the Mb derivatives exhibit a number of bands that can be assigned to out-of-plane modes by comparing their frequencies and isotope shifts to those of NiOEP<sup>4</sup> and cytochrome *c*.<sup>6</sup> Table 3 allocates these bands for metMb to the local coordinates and compares the assigned or calculated frequencies to those in NiOEP and cytochrome *c*.

The highest out-of-plane modes are expected at ~850 cm<sup>-1</sup> and involve C<sub>m</sub>-H wagging,  $\gamma(\text{C}_m-\text{H})$ . These modes are not enhanced for metMb or deoxyMb, but bands are observed at 830 and 831 cm<sup>-1</sup> for the CO and CN<sup>-</sup> adducts, which disappear in the *meso*-D<sub>4</sub> spectra. They are assigned to  $\gamma_{10}$  on the basis of the interaction with  $\gamma_{12}$  (see below).

Three pyrrole folding modes can be assigned. A pair of bands at 715 and 721 cm<sup>-1</sup> in the metMb spectrum exhibit 6- and 4-cm<sup>-1</sup> <sup>15</sup>N downshifts and are assigned to  $\gamma_{11}$  and  $\gamma_5$ . These assignments are further supported by their large *meso*-D<sub>4</sub> upshifts, from 715 to 731 cm<sup>-1</sup> for  $\gamma_{11}$  and from 721 to 774 cm<sup>-1</sup> for  $\gamma_5$  as observed in NiOEP. Interestingly,  $\gamma_5$  is also found to be particularly sensitive to the heme structure, shifting from 721 cm<sup>-1</sup> for metMb to 732 cm<sup>-1</sup> for deoxyMb and to 733 cm<sup>-1</sup> for Mb-CO. This large a frequency shift has not been seen for other low-frequency heme modes. Another pyrrole folding mode,  $\gamma_{21}$ , is assigned to a spectral feature at 547 cm<sup>-1</sup>. The marked sensitivity of the pyrrole folding modes to vinyl, methyl, and propionate deuteration reflects substantial contributions from substituent bending coordinates.

One of the pyrrole swiveling modes ( $\gamma_{12}$ , B<sub>1d</sub>) is seen at 502 cm<sup>-1</sup> for metMb, exhibiting little <sup>15</sup>N, but a large (8 cm<sup>-1</sup>) *meso*-D<sub>4</sub> shift. We note that the isotope shift pattern of  $\gamma_{12}$  is different

from that in NiOEP, but similar to that seen in cytochrome *c*. The difference has been attributed<sup>6</sup> to an altered mixing pattern between  $\gamma(\text{C}_m-\text{H})$  ( $\gamma_{10}$ ) and  $\gamma_{12}$ .

Other observed out-of-plane modes include pyrrole tilting ( $\gamma_6$  at 337 cm<sup>-1</sup>) and methine wagging ( $\gamma_7$  at 305 cm<sup>-1</sup>).  $\gamma_6$  is seen as a low-energy shoulder on a broad feature centered at 344 cm<sup>-1</sup>, the main peak being assignable to  $\nu_8$ . When *meso*-protons are exchanged with deuterium, the asymmetrical 344-cm<sup>-1</sup> band becomes symmetric and a new feature emerges at 315 cm<sup>-1</sup>. The large *meso*-D<sub>4</sub> shift (22 cm<sup>-1</sup>) agrees with that expected for  $\gamma_6$ . The 307-cm<sup>-1</sup> band had been assigned to vinyl bending<sup>7</sup> because of its sensitivity toward vinyl deuteration, but the observed *meso*-D<sub>4</sub> shift (9 cm<sup>-1</sup>) clearly favors assignment to  $\gamma_7$ . The shift seen for the 2,4-di(*b*-D<sub>2</sub>) and 6,7-di(*d*-D<sub>2</sub>) isotopomers implies substantial contributions from vinyl and methyl and/or propionate substituents, as do the even larger isotope shift seen for the  $\gamma_{12}$  pyrrole swiveling mode at 502 cm<sup>-1</sup> (Figure 6).

We note that the out-of-plane modes  $\gamma_6$ ,  $\gamma_7$ ,  $\gamma_{12}$ , and  $\gamma_{21}$  are active in the high-spin complexes metMb (Figure 6) and deoxyMb (Figure 7), but not in the low-spin adducts MbCO (Figure 9) and metMb-CN (Figure 10). This pattern is consistent with the out-of-plane intensity depending on an out-of-plane distortion of the heme group, since the Fe atoms are out of the heme plane for the high-spin complexes, but in the plane for the low-spin complexes. It is curious, however, that the  $\gamma(\text{C}_m-\text{H})$  mode  $\gamma_{10}$  (830 cm<sup>-1</sup>) is seen for Mb-CO and metMb-CN, but not for metMb or deoxyMb. The metMb-CN and Mb-CO spectra contain additional bands arising from Fe-CN (453 cm<sup>-1</sup>)<sup>14</sup> and Fe-CO (509 cm<sup>-1</sup>) stretching and Fe-C-O bending (575 cm<sup>-1</sup>),<sup>15</sup> while deoxyMb displays the well-known Fe-His stretch<sup>16</sup> at 220 cm<sup>-1</sup>.

**D. Implications.** The original assignments<sup>7</sup> by Choi et al. of vinyl modes and of vinyl effects on porphyrin modes from RR and IR spectra of isotopically labeled nickel protoporphyrin and myoglobin have been mostly confirmed in subsequent studies.<sup>12</sup> However, a few assignments were in error and are corrected in the present study, which has the benefit of high signal/noise and a larger range of isotopomers. These misassignments had suggested a strong coupling between the vinyl substituents leading to ~100 cm<sup>-1</sup> separation between modes involving the same vinyl coordinate, e.g.,  $\delta(\text{C}_\alpha\text{H}_2)$  and  $\delta(\text{C}_\beta\text{C}_\alpha\text{C}_\beta)$ . This idea was challenged by Kitagawa and co-workers<sup>12</sup> who found no evidence of large intervinylic coupling in their normal mode calculation on a model tetravinylporphyrin. The current reassignments support the absence of such an effect, although smaller differences between some nominally equivalent vinyl modes [ $\delta(\text{C}_\alpha\text{H}=\text{C}_\beta)$ ,  $\delta(\text{C}_\alpha\text{H}_2)_{\text{as}}$ , and  $\delta(\text{C}_\beta\text{C}_\alpha\text{C}_\beta)$ ] are found.

The role of vinyl orientation has been investigated by Kalsbeck et al.<sup>17</sup> who observed two  $\nu(\text{C}_\alpha=\text{C}_\beta)$  RR bands, at 1620 and 1631 cm<sup>-1</sup>, in solutions containing hemes that have either one or two vinyl substituents. The relative intensities were temperature dependent, indicating contributions from different conformers. Density functional calculations on model compounds gave two low-energy conformers with predicted  $\nu(\text{C}_\alpha=\text{C}_\beta)$  differing by 10–20 cm<sup>-1</sup>. A number of heme proteins<sup>18</sup> are reported to have two  $\nu(\text{C}_\alpha=\text{C}_\beta)$  RR bands, at

(14) Henry, E. R.; Rousseau, D. L.; Hopfield, J. J.; Noble, R. W.; Simon, S. R. *Biochemistry* **1985**, *24*, 5907–5918.

(15) Tsubaki, M.; Srivastava, R. B.; Yu, N.-T. *Biochemistry* **1982**, *21*, 1132.

(16) Stein, P.; Mitchell, M.; Spiro, T. G. *J. Am. Chem. Soc.* **1980**, *102*, 7795–7797.

(17) Kalsbeck, W. A.; Ghosh, A.; Pandey, R. K.; Smith, K. M.; Bocian, D. F. *J. Am. Chem. Soc.* **1995**, *117*, 10959–10969.

(18) Smulevich, G.; Miller, M. A.; Gosztola, D.; Spiro, T. G. *Biochemistry* **1989**, *28*, 5058–5064.



$\sim 1620$  and  $1630\text{ cm}^{-1}$ , suggesting that the two vinyl substituents have different orientations (or that a single substituent has enough flexibility in the protein to occupy alternative conformations). However, crystal structures are unavailable for these proteins. The fact that the two vinyl  $\nu(\text{C}_a=\text{C}_b)$  modes are both at  $1620\text{ cm}^{-1}$  in Mb, and also in the acid form of cytochrome *c* peroxidase,<sup>19</sup> is not inconsistent with the orientation hypothesis because the crystallographically determined  $\text{C}_\beta\text{C}_\beta\text{C}_a=\text{C}_b$  dihedral angles are all essentially the same,  $30\text{--}37^\circ$ .<sup>20</sup>

However, the orientation may not be the only relevant variable, since the compositions of the two  $\nu(\text{C}_a=\text{C}_b)$  modes are different even when these frequencies are the same. This difference is evident in the differing isotopic shifts upon selective labeling of the 2- and 4-vinyl groups in both Mb and cytochrome *c* peroxidase.<sup>19</sup> What determines these compositions is not clear. It is interesting that the 2- and 4-vinyl frequencies do diverge for other vinyl modes in Mb, i.e.,  $\delta(\text{C}_a\text{H}=\text{C}_b) = 1316/1301\text{ cm}^{-1}$ ,  $\delta(=\text{C}_b\text{H}_2)_{\text{as}} = 1092/1048\text{ cm}^{-1}$  and  $\delta(\text{C}_\beta\text{C}_a\text{C}_b) = 440/409\text{ cm}^{-1}$ . The vinyl bends are heavily mixed with methyl bends, and this mixing differs for the two vinyl-bearing pyrroles, as evidenced by different isotope shifts for the 2- and 4-vinyl-localized modes. A possible explanation of these complex effects is that out-of-plane distortions affect the pyrrole rings differently and modify the vinyl couplings to the porphyrin modes.

Effects of out-of-plane distortion are seen directly in the activation of out-of-plane porphyrin modes. The RR enhancement is derived from the coupling of heme vibrational modes to the  $\pi\text{--}\pi^*$  excitation of the B-band, which is polarized in the porphyrin plane. For out-of-plane motions, such coupling requires a static out-of-plane distortion. Evidence for this mechanism is the activity of several out-of-plane modes,  $\gamma_6$ ,

$\gamma_7$ ,  $\gamma_{12}$ , and  $\gamma_{21}$ , only in the high-spin Mb derivatives metMb and deoxyMb in which the Fe atom lies out of the average heme plane. However, additional porphyrin distortion is implied by the activation even in the low-spin adducts of other out-of-plane modes,  $\gamma_5$ ,  $\gamma_{10}$ , and  $\gamma_{11}$ .

It is interesting to contrast the influence of the protein on the RR spectrum of Mb and cytochrome *c*. The heme in cytochrome *c* is covalently bound to the protein and is subject to a pronounced propeller distortion of the porphyrin skeleton.<sup>21</sup> One consequence of this is activation of anomalously polarized bond-alternant  $\text{A}_{2g}$  modes with B-band excitation. Such modes are not normally seen in the B-band-excited RR spectra of metalloporphyrins and are not observed for Mb. Another effect was strong activation of the pyrrole folding mode  $\gamma_{12}$ , even though cytochrome *c* is low spin. In Mb, only the high-spin forms show  $\gamma_{12}$  activation. On the other hand, the pyrrole and methine wagging modes  $\gamma_6$  and  $\gamma_7$  were not seen in cytochrome *c*, but are activated in high-spin Mb derivative. These modes apparently require out-of-plane displacement of the metal for their activation. Thus, distinctive differences in protein-specific effects can be detected in the RR spectra.

**Acknowledgment.** This work was supported by NIH Grants GM33576 (to T.G.S.) and HL 22252 (to K.M.S.).

JA962239E

(19) Smulevich, G.; Hu, S.; Rodgers, K. R.; Goodin, D. B.; Smith, K. M.; Spiro, T. G. *Biospectroscopy*, in press.

(20) Reid, L. S.; Lim, A. R.; Mauk, A. G. *J. Am. Chem. Soc.* **1986**, *108*, 8197–8201.

(21) (a) Dickerson, R. E.; Kopka, M. L.; Borders, C. L., Jr.; Varnum, J. C.; Weinzierl, J. E.; Margoliash, E. *J. Mol. Biol.* **1967**, *29*, 77–95. (b) Dickerson, R. E.; Kopka, M. L.; Weinzierl, J. E.; Varnum, J. C.; Eisenberg, D.; Margoliash, E. *J. Biol. Chem.* **1967**, *242*, 3015–3018. (c) Takano, T.; Kallai, O. B.; Swanson, R.; Dickerson, R. E. *J. Biol. Chem.* **1973**, *248*, 5234–5255. (d) Takano, T.; Dickerson, R. E. *J. Mol. Biol.* **1981**, *153*, 79–94. (e) Takano, T.; Dickerson, R. E. *J. Mol. Biol.* **1981**, *153*, 95–115. (f) Louie, G.; Brayer, G. D. *J. Mol. Biol.* **1990**, *214*, 527–555. (g) Berghuis, A. M.; Brayer, G. D. *J. Mol. Biol.* **1992**, *223*, 959–976.

(22) Streckas, T. C.; Packer, A. J.; Spiro, T. G. *J. Raman Spectrosc.* **1973**, *1*, 197–206.